RECEIVED BY DTIE JAN 24 1972

Coo ~~CU~~-3150-83

MASTER

GENERATION AND DETECTION OF 55 GHz PHONONS USING PARAELECTRIC RESONANCE OF KCl:Li

T. R. Larson and R. H. Silsbee

Laboratory of Atomic and Solid State Physics
Cornell University
Ithaca, New York 14850

December 1971

RECEIVED
JAN 13 1972
NEW YORK PATENT GROUP

Issued by

The Materials Science Center

Report #1700

There is no objection from the patent point of view to the publication or dissemination of this document.

Patent Group (Brookhaven)

By..........

........1/17........1972

DISTRIBUTION OF THIS DOCUMENT IS UNLIMITED

Generation and Detection of 55 GHz Phonons Using Paraelectric Resonance of KCl:Li *

T. R. Larson† and R. H. Silsbee

Laboratory of Atomic and Solid State Physics
Cornell University
Ithaca, New York 14850

ABSTRACT

Paraelectric resonance (PER) of the off-center KCl:Li system has been used both to generate and to detect phonons at microwave frequencies. Lithium was diffusion doped into both ends of a 1 x 1 x 10 mm KCl crystal, which was then placed at 1.5 K with each end protruding into a separate PER cavity. Phonons were generated at one end by a one microsecond 250 mW peak microwave pulse, and detected a time of flight later by monitoring the PER signal from the other cavity. Various phonon modes were identified by their time of flight and were studied as a function of crystal orientation, microwave power, applied dc electric field, surface preparation, and frequency separation between cavities. A change in resonant phonon temperature of 1% at the detecting end was produced. The phonon bandwidth was > six GHz in every case. The resonant

phonons are thought to undergo both spatial and spectral diffusion in the doped regions of the sample.

INTRODUCTION

KCl, doped in the one to one hundred ppm molecular range with lithium, has been extensively studied by several methods.[1] The singly ionized lithium goes in substitutionally for a K^+ ion, and occupies a complicated local potential characterized by eight minima lying off-center from the K^+ lattice site along the crystalline [111] directions. The tunneling model[2] proposed by Gomez, Bowen, and Krumhansl (GBK), assuming cube edge tunneling only, adequately describes this lithium site.

A large permanent electric dipole moment of 5.6[3] Debye (uncorrected for local field) gives the lithium ion a strong interaction with both dc and microwave electric fields. It also interacts strongly with distortions of the host KCl lattice, having a large coupling coefficient to T_{2g} symmetry lattice strain,[4] and an individual site relaxation time $T_1 \lesssim 10^{-8}$ second.[5,6] These two properties make this system a likely candidate to use as a transducer to generate microwave phonons in KCl. Channin, et al.,[7] drove this Li:LCl system with 24 GHz microwaves, and detected the resulting phonons with a superconducting bolometer but with an inherent lack of spectral resolution.

As described in the GBK model, the eight low lying energy levels of the lithium ion can be tuned with an applied dc electric field. Paraelectric resonance (PER) is the study of the microwave absorption which occurs when the energy difference between two or more of these levels corresponds to the frequency of the applied microwave radiation. The strength of this PER signal is proportional to the difference in populations of the lower and excited lithium states, and this population difference is determined by the temperature of the lattice phonons in resonance with the transition. Thus this KCl:Li system can serve as a detector of resonant phonons. Further, the use of a source and detector at different frequencies can give information on the spectral width of the generated phonons.

In the experiments reported here, both ends of a long thin KCl crystal were diffusion doped with lithium, and each end protruded into a separate PER microwave cavity. The normal PER signals from each cavity separately were used as a sensitivity calibration. By generating phonons for a time short compared to the phonon transit time down the sample, and detecting the resulting phonon flux this transit time later, effects of direct microwave feed through could be avoided.

A closely related but complementary experiment, in which the phonons are generated by application of a short pulse of a large electric field and detected by a bolometric technique, is described by Goubau in the accompanying article.[6]

APPARATUS AND PROCEDURE

As shown in figure 1, two identical $TE_{1,0,\sim5}$ microwave cavities were used, milled from a solid piece of OFHC copper. The sample fitted in a $1mm^2$ cross section channel cut between the cavities and protruded into each. The copper walls of the channel formed a guide beyond cut-off, and along with an indium gasket gave at least forty db isolation between cavities. The solid block was split along the plane shown by a dashed line in figure 1 for loading and access to the cavity interiors. A dc electric field could be applied across each end of the lithium doped sample which was between the electrode shown and the cavity wall. The geometry gave $E_{dc} \| E_{microwave}$. The electrodes were dipped in dilute GE 7031 varnish and wrapped with two mils of mylar tape, giving a useable electric field of up to 50 kV/cm without electrical breakdown. A stycast (ϵ = 10) tuning element was suspended from teflon spaghetti into each cavity and was movable during a run. Between runs, coupling to each cavity could be adjusted using the quartz rods shown.

Using a conventional microwave spectrometer, PER traces were taken for each cavity, modulating the applied dc field at

5 kHz and using lock in detection. This gave a sensitivity standard, as filling factor changed with frequency, and allowed one to tune for pure absorption. In all cases, the sample was run immersed in liquid helium below T_λ where bubbling was not a problem. The lowest temperature obtainable was 1.5 K. To look for phonons, one cavity, the pump cavity, was pulsed with up to 250 mW of microwaves for a time the order of a microsecond. The other, the detector cavity, was connected to the microwave spectrometer. With it, the reflected microwave voltage from the detector cavity was carefully monitored at a time after the pump pulse roughly equal to a phonon transit time. This was repeated at a repetition rate of about 20 kHz, and a gated integrator (boxcar) was used to improve signal to noise. Figure 2 illustrates the apparatus. Δf, the frequency separation between pump and detection frequencies, was varied from 0 to 6 GHz.

SAMPLE

The Cornell Crystal Growing Facility used Mallinckrodt analytic reagent grade KCl, bubbled it in the melt with Cl_2 gas to remove impurities, OH in particular, and pulled single crystals using the Kyropoulos technique. OH impurities would be troublesome since they have a permanent electric dipole moment and a lattice strain interaction coefficient comparable to those of lithium. Crystals were string sawn or cleaved to about 1 x 2 x 2 cm^3, with the short dimension lying along the final desired direction of propagation. Using the known diffusion constant as a function of temperature,[8] lithium was diffused in from all sides aiming for a concentration profile

$$C(x) = C_o \operatorname{erfc} [x/(4D\ t)^{\frac{1}{2}}], \tag{1}$$

down by a factor of 100 at x ≡ penetration distance from the surface = x_o, usually ½ or 1 mm. The above expression assumes a constant lithium concentration at the surface throughout the diffusion process, and was verified by Hanson, with C_o falling in the range $(7 \pm 3) \times 10^{17}\ \mathrm{Li/cm}^3$. Following Hanson, a double furnace and a sealed quartz tube were used, one section containing a mixture of 10% LiCl and 90% KCl and kept well above the melting point of either, and the other section containing the sample at a controlled diffusion temperature. At the end of the correct diffusion time at the diffusion temperature of about 600°C, forced air was used to cool the LiCl section to almost room temperature, and the sample section to 400°C, where it was kept for several hours, then cooled to room temperature at 100 degrees/hour.

From the center of this crystal the final sample of dimensions 1 x 1 x 8 to 10 mm^3 was cleaved for the long dimension along

[100], and string sawn and ground for the long dimension along [1$\bar{1}$0]. In the latter case, the sample was ground to final size with #600 carborundum followed by garnet powder. A standard etching procedure, applied in some cases, consisted of dipping in concentrated HCl for one minute, followed by pyridine, acetone, and chloroform in that order.

Prior to running, every sample was given a standard annealing procedure consisting of at least 24 hours at 400°C in a vacuum inside a pure KCl container, a cool to room temperature at 100 degrees/hour, and cooling to T_{nitrogen} within 6 hours. The careful attention to annealing was designed to reduce inhomogeneous strain broadening of the PER absorption lines.[4]

RESULTS

Figure 3 shows a typical phonon transmission signal obtained for $E_{dc} \| E_{\text{microwave}} \| [001]$ with the phonon propagation direction along [100]. After diffusion doping aiming for $x_o = 1$ mm, the sample was cleaved and given the standard anneal. The surfaces were untreated. The derivative peak to peak PER linewidth was $\simeq$ 30 GHz. The shorter sample length of 8 mm caused the doped regions to be not centered under the cavity electrodes. Besides the well documented inhomogeneous strain broadening, static field fringing probably contributed to the breadth of the PER traces, especially the asymmetric high field broadening, since the PER traces of Herendeen and Silsbee[3] were a factor of 5 narrower.

Note that the ballistic phonon arrival times, given by the leading edges of the linear sections of the phonon signal, correspond to the expected times L/v_ℓ and L/v_t, where v_ℓ and v_t are the known longitudinal and transverse sound velocities, respectively, and L is the sample length. Two months in a desiccator at room temperature followed by another standard anneal had no effect on either the PER or phonon signals.

The phonon signal for $E_{dc} \| E_{microwave} \| [111]$, direction of propagation along $[1\bar{1}0]$, is shown in figure 4. Sample length was 10 mm and the estimated x_o was ½ mm. The derivative peak to peak PER linewidth was also $\simeq$ 30 GHz, even though the electric field was more homogeneous than for [100], presumably because inhomogeneous static strain broadening is expected to be considerably worse for this orientation.[3] For the $[1\bar{1}0]$ direction of propagation, four arrival times are expected, as will be discussed below. These are indicated in figure 4.

The phonon signal strength varied dramatically with surface preparation in the case of this sample with $E \| [111]$, the signal being observed only under these conditions: careful grinding, the standard anneal, and then the etch procedure, all as described under sample preparation. Phonon signal deterioration with time was observed. A "good" [111] sample was left at room temperature in a desiccator for two months and then re-measured, with no phonon signal observable, i.e. the signal was down by at least a factor of 10^3. (The PER signals were unchanged, for all the situations described here.) Re-annealing had no effect on the phonon signal. A re-etch, however, returned a phonon signal, but smaller by about a factor of 5 than the original run. Subsequent re-etches again produced no observable phonon signal. Surface quality, observed under 30X magnification, deteriorated with each subsequent etch. One could postulate that the etching procedure was only effective on freshly ground level surfaces. Subsequent etchings produced microscopic undulations of length the order of one mil, and these were amplified by each succeeding etch. In every case where no phonon signal was observed, the function of the two cavities was switched during the search to eliminate, for example, any stray effect deteriorating a cavity's efficiency as a generator but not a detector.

For both orientations, the peak phonon signal observed was a maximum of about 1% of the PER signal which would be obtained by modulating the entire linewidth. Also for both orientations, no experimentally significant variation of phonon signal shape (in time) or intensity (to within a factor of 3 or 4) was observed for $0 \leq \Delta f < 6$ GHz, where Δf is the difference between generating and detecting microwave frequencies, and the 6 GHz upper bound was determined by our klystrons.

Besides the agreement of the arrival times with predicted values, a number of tests performed gave conclusive evidence that the phonon signal, the change in the PER signal at the detector cavity, was due in fact to phonons generated at the other end of the sample. In every case where a phonon signal was observed, and at every observed Δf, the peak phonon signal amplitude varied linearly with input microwave pump pulse power, as shown in figure 5. For pump pulse lengths appreciably shorter than the phonon transit time, so that the phonon signal shape becomes largely independent of pump pulse length, the peak phonon signal amplitude scaled linearly with pump pulse length, as shown in figure 6. To restate, for this range of pump pulse lengths, the total energy put into the pump cavity to generate phonons is equal to the pump pulse power times the pump pulse length, and the observed behavior is that the peak phonon signal scales linearly with either of these parameters, for both orientations and all Δf's.

As a final test, the peak phonon signal is shown in figure 7 as a function of the applied dc field in the pump cavity, for the [001] orientation, superposed on the pump cavity derivative PER signal. A very similar variation in peak phonon signal with pump E_{dc} was observed for the [111] orientation. Note the coinciding center field and width.

The effect on the peak phonon signal of varying the detector electric field depended markedly on the tuning of the microwave phase of the PER spectrometer. By carefully tuning for absorption using the equal-lobed PER signal as a criterion, and then observing the peak phonon signal as a function of the detector electric field, qualitatively the same behaviour was observed, for both orientations, as that shown in figure 7.

No evidence of saturation was seen in normal PER measurements made at 1.6 K using one of these cavities and the [100] sample. The crudely estimated maximum power incident on the cavity was 50 mW, with about 5% of this being absorbed by the sample. The linear scaling of the peak phonon signal with input pump power, mentioned earlier, also indicates no appreciable saturation up to the maximum pump power of 250 mW.

DISCUSSION

A simple interpretation of these experiments, as of those of Channin et al.,[7] is that the microwave pulse via photon excitation and phonon relaxation at the lithium sites heats the phonons in a bandwidth $1/T_1$ about the exciting microwave frequency at the source end of the crystal. This hot band of phonons, after propagating to the detector end of the crystal, heats the lithium whose PER is being monitored. The decrease in PER signal induced by this heating may be monitored as a function of the frequency separation of the source and detector klystrons to obtain a measure of the spectral breadth of the transmitted phonons.

This naive picture of the process suggests that the transmitted signal should fall off as the frequency separation becomes greater than $1/T_1$, the predicted bandwidth of the emitted phonons. This prediction is in strong contradiction with the experiment which showed apparently comparable signal magnitude for frequency separations as large as 6 GHz while estimates of $\frac{1}{2\pi T_1}$ are in the range 10^{-2} to 10^{-1} GHz. A more careful look at the details of the escape of the phonons from the source region shows that the picture of simple photon absorption with subsequent phonon emission into the bulk of the crystal is unrealistic. The very strong coupling between the phonons and the lithium impurities implies, as is shown below, that at typical experimental concentrations the phonons are strongly trapped in the source region and are able to escape only after many absorptions and reemissions by the lithium centers.

Similar considerations to those below should be applied to the discussion of the fate of those heated phonons which arrive at the detector region. Since the full discussion of the experiment is remarkably symmetric in the details of what occurs in the source and detector regions, the following remarks are restricted for convenience only to the source, and should be appropriately translated to the detector region for a complete picture of the experiment.

The apparent severity of the bottlenecking problem is illustrated by using the usual detailed balance argument to estimate the mean life of a phonon between emission by one lithium and absorption by another. Equating the rate of upward lithium transitions $\sim (N/2T_1)$ (assuming $kT > \hbar\omega$) to the rate of phonon absorption processes $\sim (p\ \rho(\omega)\ \Delta\omega/t_p)$, where p is the phonon occupation number, $\rho(\omega)$ the phonon density of states, $\Delta\omega$ the inhomogeneous bandwidth of the lithium PER and t_p the lifetime of a phonon against absorption, one estimates $t_p \sim 2 \times 10^{-10}$ sec for a lithium concentration of 10^{18} cm^{-3} and a T_1 of 10^{-9} sec, parameters that will be used for all of the following very rough estimates. This time is of course very short compared with the free flight transit time, 4×10^{-7} sec, across the 1 mm doped region. The random walk time for escape from the doped region may be roughly estimated from this scattering time and the size D of the region as

$$\tau_{\text{spatial}} \sim (T_1 + t_p)(D/2\ vt_p)^2 \sim 10^{-3}\ \text{sec.}$$

The experiments show, however, arrival of essentially the full pulse within roughly ten microseconds, with a leading edge which extrapolates to the ballistic arrival time at zero intensity. Whether the delay to the peak of the pulse of a few to ten microseconds is associated with diffusion of the hot phonons out of the source region or with diffusive transport down the length of the sample via successive wall collisions was not established in these experiments. In any case, the pulse arrives in a time quite short compared with the estimate above of one millisecond, indicating the presence of a mechanism of escape from the source which is more rapid than the simple spatial diffusion.

A second important consequence of multiple collisions within the source region is that the frequency bandwidth of the heated phonons may become much greater than the naive estimate of $1/T_1$ based on the assumption of no multiple phonon scattering. If the level splittings of the lithium ion are smaller than or comparable with kT, as they were in this experiment, there are two important mechanisms for this spectral diffusion. First, each time a phonon is absorbed and reemitted the frequency after emission may be shifted from that before emission by an amount the order of $1/T_1$, the lifetime breadth of the lithium levels. The spectral step length may be greater than $1/T_1$ due to interactions between centers or any other mechanisms contributing to a homogeneous width, but the crudity of the present arguments hardly warrants consideration of such fine points. In addition, because of the complex level structure of the lithium tunneling states the return of the lithium to equilibrium may be achieved by emitting phonons not only of frequency nearly that of the incident microwaves but also at frequencies corresponding to others of the level splittings of figure 8, i.e. multiples of the microwave frequency and/or sums and differences of these multiples and the zero field splittings, depending upon the specific sample orientation in question.

Using a random walk argument to estimate the effect of the first mechanism, the time for diffusion through the full inhomogeneous breadth of the line is

$$\tau_{\text{spectral}} \sim (T_1 + t_p)\left(T_1\Delta\omega/2\right)^2 \sim 5 \times 10^{-6} \text{ sec.}$$

Noting that this time is significantly shorter than that estimated for the spatial diffusion suggests that much of the excess energy delivered to the crystal by the microwave pulse leaves the source region first by a spectral diffusion mechanism to a region of the phonon spectrum where the material is more transparent, and then spatial diffusion out of the source region, the spatial diffusion being more rapid in the nearly transparent wings of the inhomogeneous line.

It is possible that the most important mechanism for the transport of energy out of the source region is in fact via those phonons which are in resonance with the higher frequency transitions of the centers, the second mechanism mentioned above. The higher mode density at the higher frequencies implies a less severe bottleneck for these phonons and the spectral diffusion time estimated above of $\sim 5 \times 10^{-6}$ sec should be correspondingly shortened.

This estimate of the time for spectral diffusion is comparable with the observed peak delays, suggesting that the breadth of the pulses may be associated with the diffusion of the phonons out of the source. The estimates are too unreliable to eliminate the possibility that the delay is the result of the restriction of the transport down the crystal by partially diffusive wall collisions, the escape from the source region being rapid compared with the experimental resolution time.

Further evidence of the absence of a severe phonon bottleneck is the lack of saturation of the PER at a power level into the cavity of 20 mW and the absence of saturation of the transmitted phonon signal at pulse powers to the cavity of 250 mW. This absence of saturation seems consistent only with a picture in which there is very rapid distribution of the microwave energy over a wide portion of the microwave spectrum.

The broad spectral width observed at the detector might also be interpreted as a consequence of inelastic scattering of the phonons from the surfaces of the sample, since it is thought that a substantial portion of the observed signal is associated with phonons which have undergone one or several wall collisions during transit of the crystal. It does not seem possible to attribute the breadth solely to this mechanism, however, since both the absence of saturation of the PER and the absence of a pulse delay of the order of a millisecond as estimated for the spatial diffusion of monochromatic phonons indicate the need for substantial spectral broadening.

It should be emphasized that the two spectral diffusion mechanisms discussed above, successive scatterings of the phonons, with spectral shifts $\sim (1/T_1)$ at each scattering, and equilibration of the levels through higher frequency phonons, are both suppressed when one lowers the temperature to values very small compared with the level splitting. In absence of thermal phonons, the successive scattering process should be thought of as a resonance fluorescence in which there is no broadening of the radiation upon scattering;[9] in fact the heated phonon bandwidth in this low temperature limit is just the microwave bandwidth since the conversion of photon to phonon should itself be thought of as a resonance fluorescence process. Also the equilibration through higher frequency processes depends upon this presence of thermal phonons and upon the thermal excitation of the lithium centers out of the ground state and is therefore suppressed in the low temperature limit. Thus there seems strong motivation for studying the properties of the system at lower temperatures where the rapid spectral equilibration should be absent.

Rough estimates are possible of the magnitude of the change in temperature produced by the ballistically transmitted phonons by comparison of the magnitude of the change in PER in the transmission experiment with the amplitude of the normal PER signal, making appropriate correction for the modulation amplitude used in the derivative recording of the PER. In the sample with the largest signals, the change in temperature at the detector was about 1% of the ambient temperature (~ 1.5 K) for a pump pulse of 250 mW to the transmitter cavity of duration 1/2 μ sec. Estimates of cavity Q and geometry and use of the known dipole moment for the transition give a value of dissipation of about 20 mW in the source end of the crystal or a pulse energy of 10^{-1} ergs. Noting that the specific heat at the detector end of the crystal is dominated by the lithium centers gives an estimate of 2×10^{-3} ergs for the excess energy content in this end of the crystal at the peak of the transmitted pulse or about 2% of the energy deposited in the source by the microwave pulse. Depending upon one's interpretation of the observed pulse widths, as being the result of trapping within the source and detector regions or the consequence of partially diffusive transport along the crystal, the total fraction of the incident microwave pulse energy which reaches the detector region is estimated to be in the range a few per cent to the order of one half. These numbers are surely accurate to no more than a factor of three, but they serve to emphasize a substantial efficiency of conversion and transport.

In principle one should be able to estimate the relative amount of energy carried by each of the acoustic needs, the two relevant modes for the [100] propagation being reasonably resolved for the [100] data. The relative contribution to the pulse height of a given symmetry of modes, assuming all are heated to the same degree, is proportional to the energy flux carried by the individual mode ($\sim v$), the number of such modes within the heated bandwidth ($\sim 1/v^3$), and a factor related to the focussing[10] of phonons associated with the elastic anisotropies of the crystal. For the [100] sample, the comparable intensities of the two components is consistent with these considerations. For the [110] propagation there are not clearly resolved components and the fast components seem relatively weaker than one would expect. It is possible that in this crystal, with ground, polished and etched surfaces as opposed to the cleaved surfaces of the [100] sample, there was substantial mode mixing at the imperfect surface to give a single ill defined transit time determined by an average sound velocity. Note that in this case, the average sound velocity is dominated by the slower modes; the simple average should be of the inverse sound velocities.

If the proposal above, that there is multiple scattering of the phonon before release from the source, is correct then the selection rules for the transitions are <u>not</u> relevant to the observed intensities for much the same reason that the selection rules are not relevant to the intensity of optical emission from a gas at those frequencies for which the gas is optically dense; at any frequency for which the source in equilibrium is optically dense, the emission intensity is that of a black body at that same temperature. This is the one point in which the interpretation of these experiments is in contradiction with the results of Channin, et al., who seem to have demonstrated a substantial effect of the selection rules. This contradiction is not resolved here.

CONCLUSION

PER of the off center lithium ion was used both to generate and to detect 52 to 58 GHz phonons in KCl. Two orientations were used, $E_{dc} \| E_{microwave} \| [001]$ and [111], having the direction of propagation along [100] and [$1\bar{1}0$] respectively. The phonons, generated using a pulsed klystron with a bandwidth the order of 1 MHz, had a bandwidth of at least 6 GHz for both orientations. This bandwidth, the order of the lithium inhomogeneous linewidth, would be produced when the phonons undergo spectral diffusion via multiple collisions with the lithium sites before leaving the generating region. The time for generated phonons to diffuse to the edge of the generating region is estimated by a simple diffusion calculation for both spectral and spatial diffusion processes. Spatial diffusion alone cannot account for the emission times observed. Efforts to saturate the [001] sample were unsuccessful, and can only be explained by the possibility of spectral diffusion and phonon relaxation via other transitions between energy levels besides the microwave driven ones.

REFERENCES

* This work has been supported by the U. S. Atomic Energy Commission under Contract No. AT(11-1)-3150, Technical Report No. CH-3150-83. Additional support was received from the Advanced Research Projects Agency through the Materials Science Center at Cornell University, Report No. 1700.

† Present address: Naval Research Laboratory, Washington, D. C. 20390.

1. V. Narayanamurti and R. O. Pohl, Rev. Mod. Phys. 42, 201 (1970).
2. M. Gomez, S. P. Bowen, and J. A. Krumhansl, Phys. Rev. 153, 1009 (1967).
3. R. A. Herendeen and R. H. Silsbee, Phys. Rev. 188, 645 (1969).
4. T. R. Larson and R. H. Silsbee, (to be published) Phys. Rev. 5B, January 1972.
5. S. Kapphan and F. Lüty, S. S. Comm. 6, 907 (1968).
6. W. M. Goubau, Phys. Rev., this issue.
7. D. J. Channin, V. Narayanamurti and R. O. Pohl, Phys. Rev. Letters 22, 524 (1969).
8. R. C. Hanson, Phys. Stat. Sol. (a) 1, 109 (1970).

9. D. J. Channin, unpublished thesis; Cornell Materials Science Center Report #1311 (1970).

10. B. Taylor, H. J. Maris and C. Elbaum, Phys. Rev. B3, 1462 (1971).

FIGURE CAPTIONS

Fig. 1: Identical tunable PER cavities used to generate and detect 52 - 58 GHz phonons traversing the 1 x 1 x 8-10 mm^3 KCl sample which was doped at both ends with lithium.

Fig. 2: Apparatus diagram, showing pulsed pump klystron used to produce phonons in the generator cavity, and the spectrometer used to monitor changes in reflected microwave power from the detector cavity.

Fig. 3: Changes in PER signal from the detector cavity as a function of time after pump klystron was pulsed, $v_g \| [100]$, $E_{dc} \| E_{microwave} \| [001]$. The peak phonon signal was ~ 1% of the normal PER signal which would be produced by modulating the entire linewidth. No appreciable change in shape or intensity was seen for 0 < frequency difference between cavities < 6 GHz.

Fig. 4: Change in detector cavity PER signal as a function of time after pump klystron was pulsed, $v_g \| [1\bar{1}0]$, $E_{dc} \| E_{microwave} \| [111]$. The peak phonon signal was ~ 1% of the PER signal which would be produced by modulating the entire linewidth. No appreciable change in shape or intensity was seen for 0 < frequency difference between cavities < 6 GHz.

Fig. 5: Peak phonon signal vs. relative pump pulse power for both orientations and for all values of the frequency difference between cavities up to 6 GHz.

Fig. 6: Peak phonon signal vs. pump pulse width, $E_{dc} \| E_{microwave} \| [001]$, $v_g \| [100]$ and for all values of the frequency difference between cavities up to 6 GHz. Similar behavior was observed for the other orientation studied.

Fig. 7: Peak phonon signal vs. dc electric field in pump cavity (top), to be compared with <u>derivative</u> PER signal from pump cavity vs. the same electric field (bottom). Similar behavior was observed for both orientations.

Fig. 8: Energy levels of the ground state multiplet of KCl:Li as a function of the applied static electric field as predicted by the GBK model using only the cube edge tunneling. The arrow indicates one of the allowed microwave transitions at 55 GHz if Δ is taken as 23.1 GHz.

a) $E_{dc} \| [001]$ b) $E_{dc} \| [111]$

Cavity Design

f = 52 to 58 GHz

Sample Size = 1x1x10 mm^3

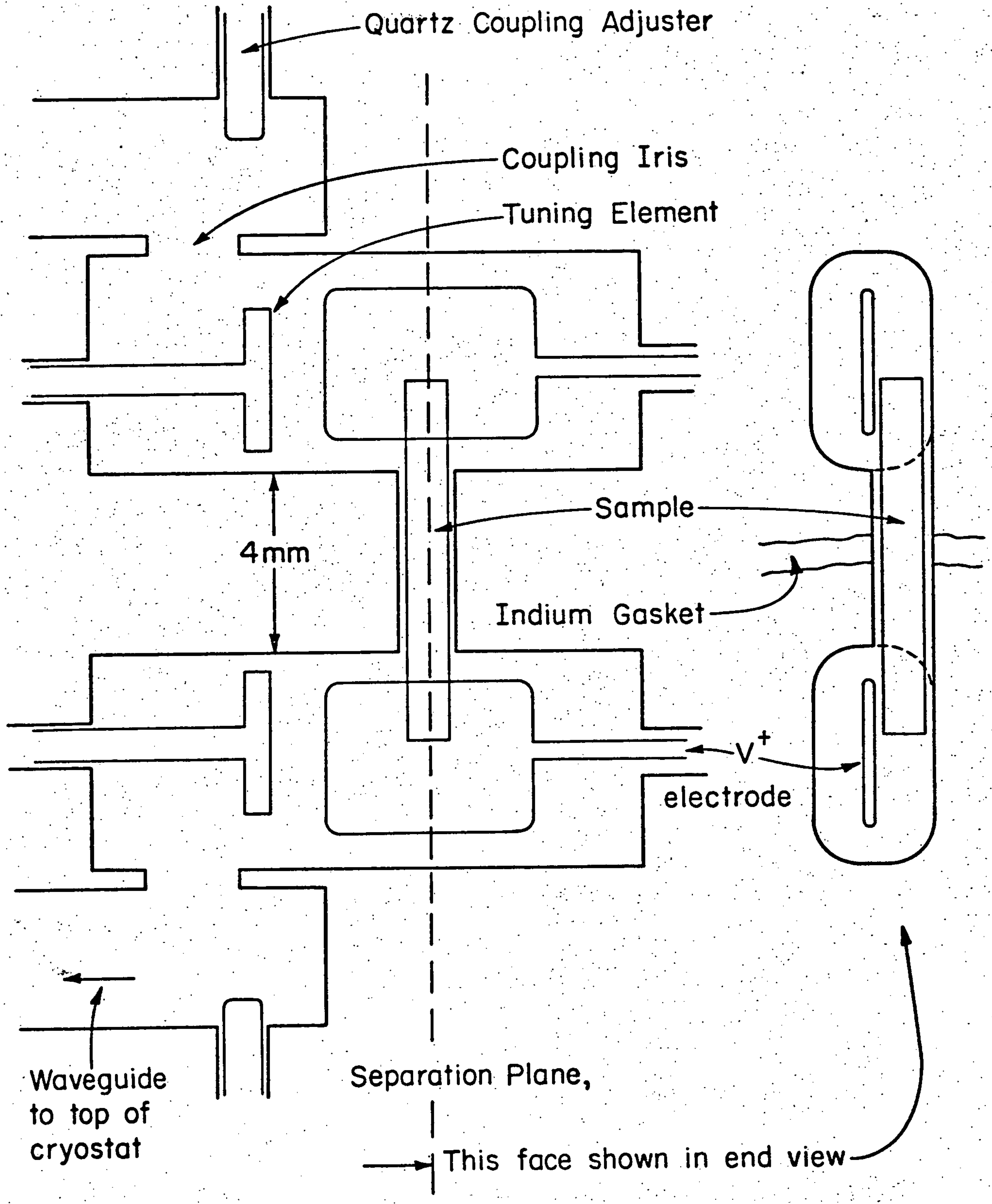

Figure 1.

SPECTROMETER

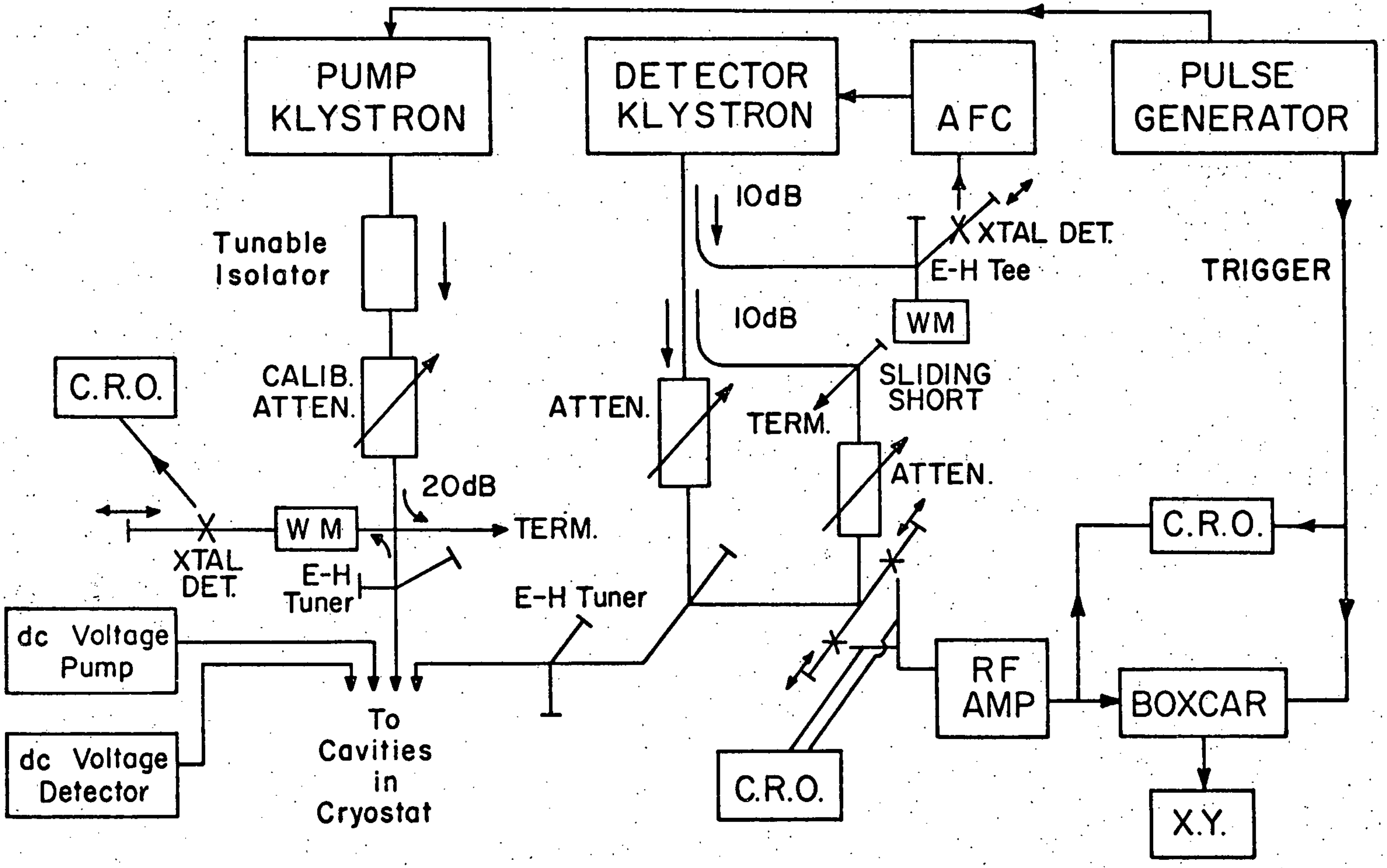

Figure 2.

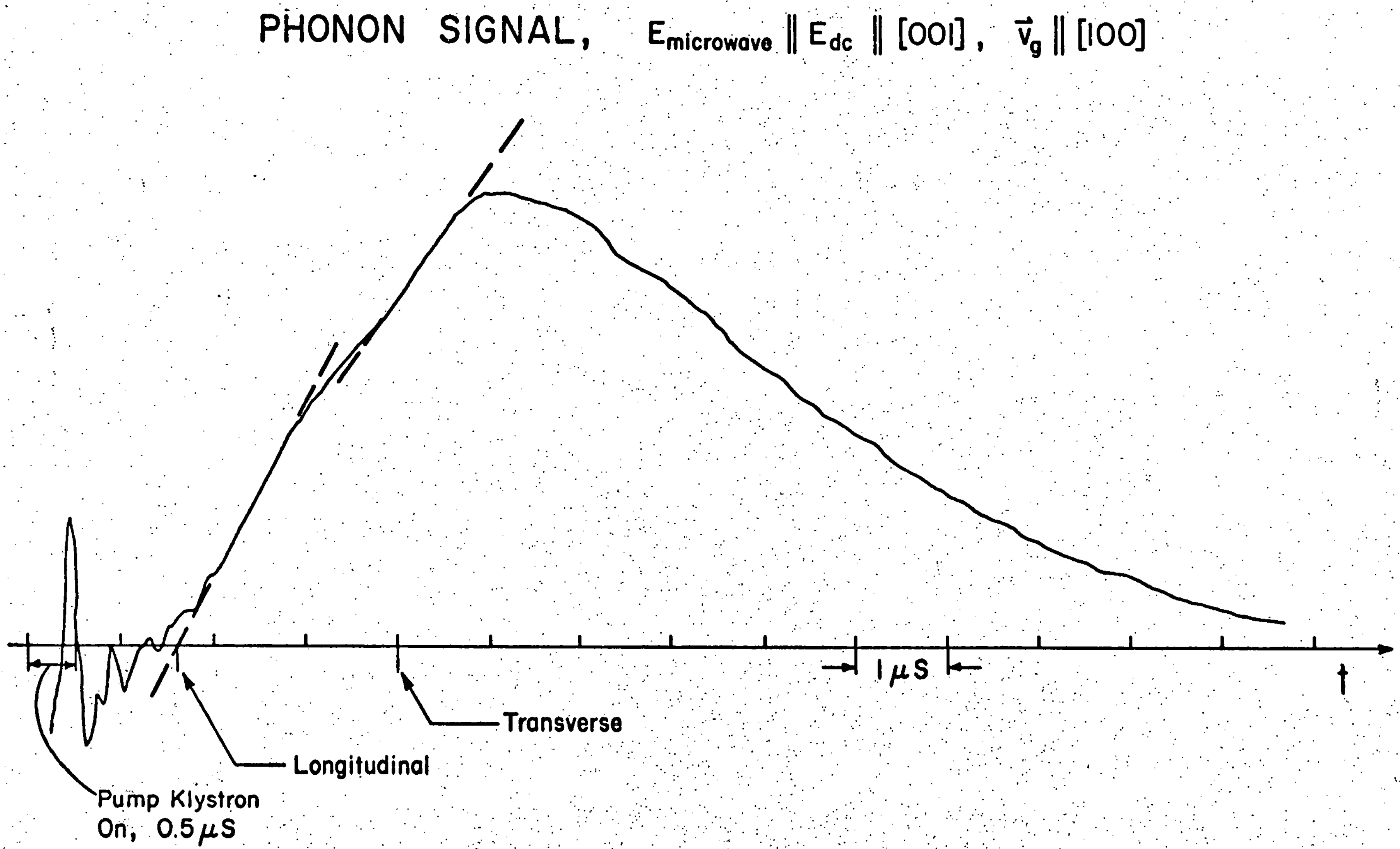

PHONON SIGNAL, $E_{microwave} \parallel E_{dc} \parallel [001]$, $\vec{v}_g \parallel [100]$

Figure 3.

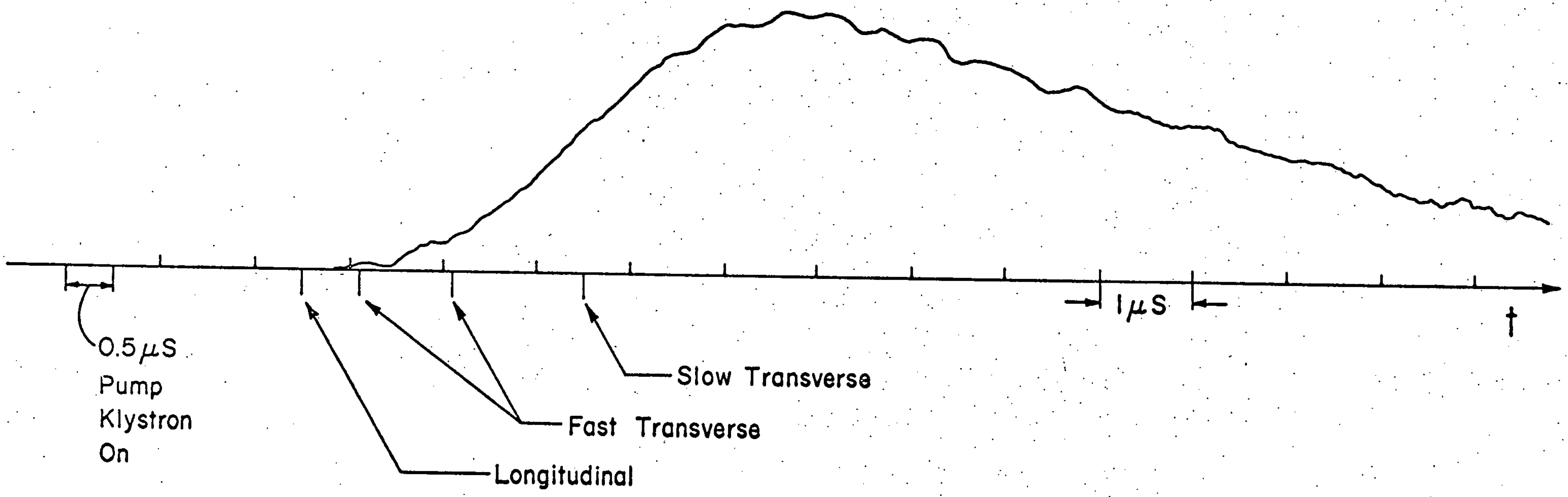

PHONON SIGNAL, $E_{microwave} \parallel E_{dc} \parallel [111]$

$\vec{v}_g \parallel [1\bar{1}0]$

Figure 4.

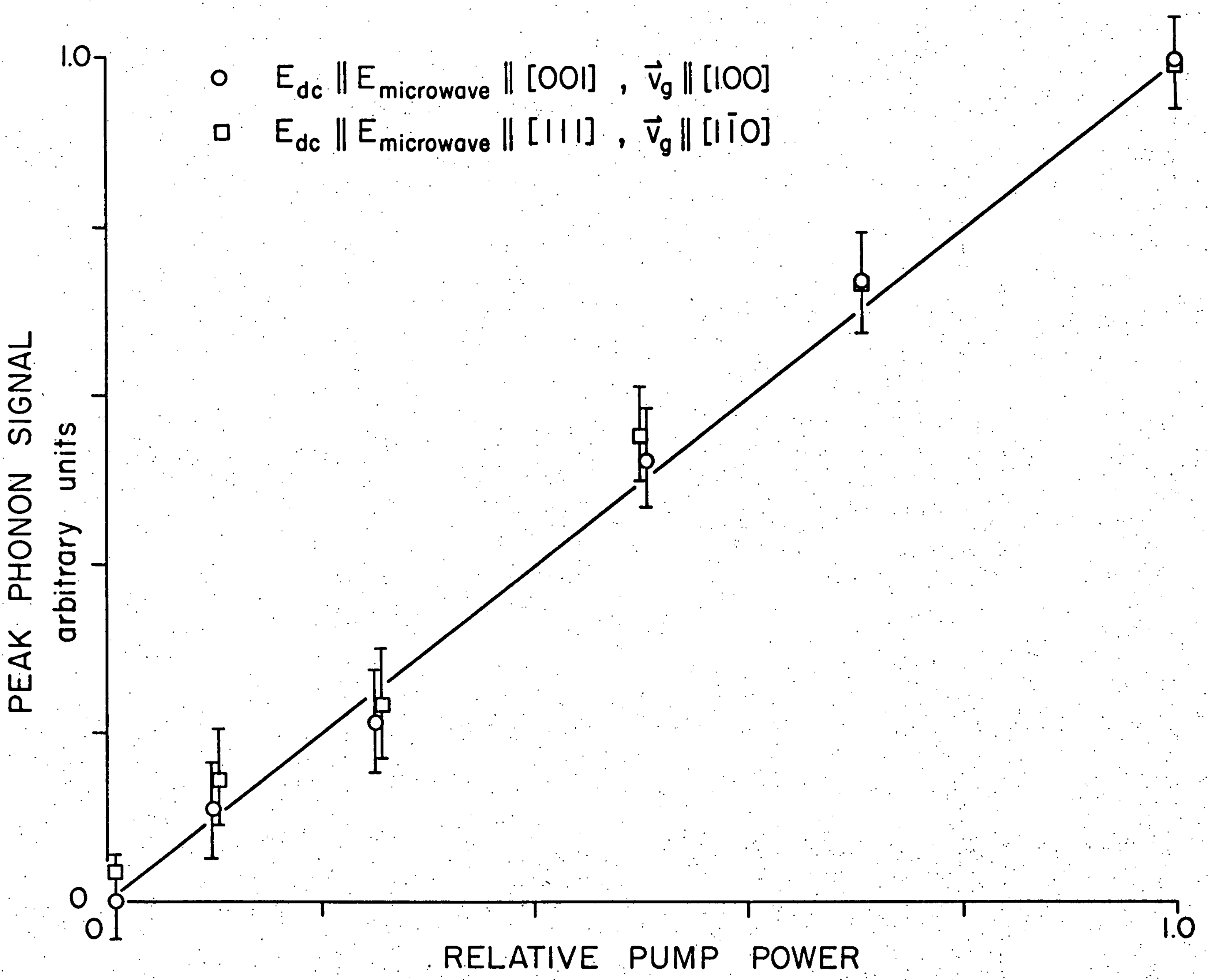
1.0
0
0
1.0
○ $E_{dc} \parallel E_{microwave} \parallel [001]$, $\vec{v}_g \parallel [100]$
□ $E_{dc} \parallel E_{microwave} \parallel [111]$, $\vec{v}_g \parallel [1\bar{1}0]$
PEAK PHONON SIGNAL
arbitrary units
RELATIVE PUMP POWER

Figure 5.

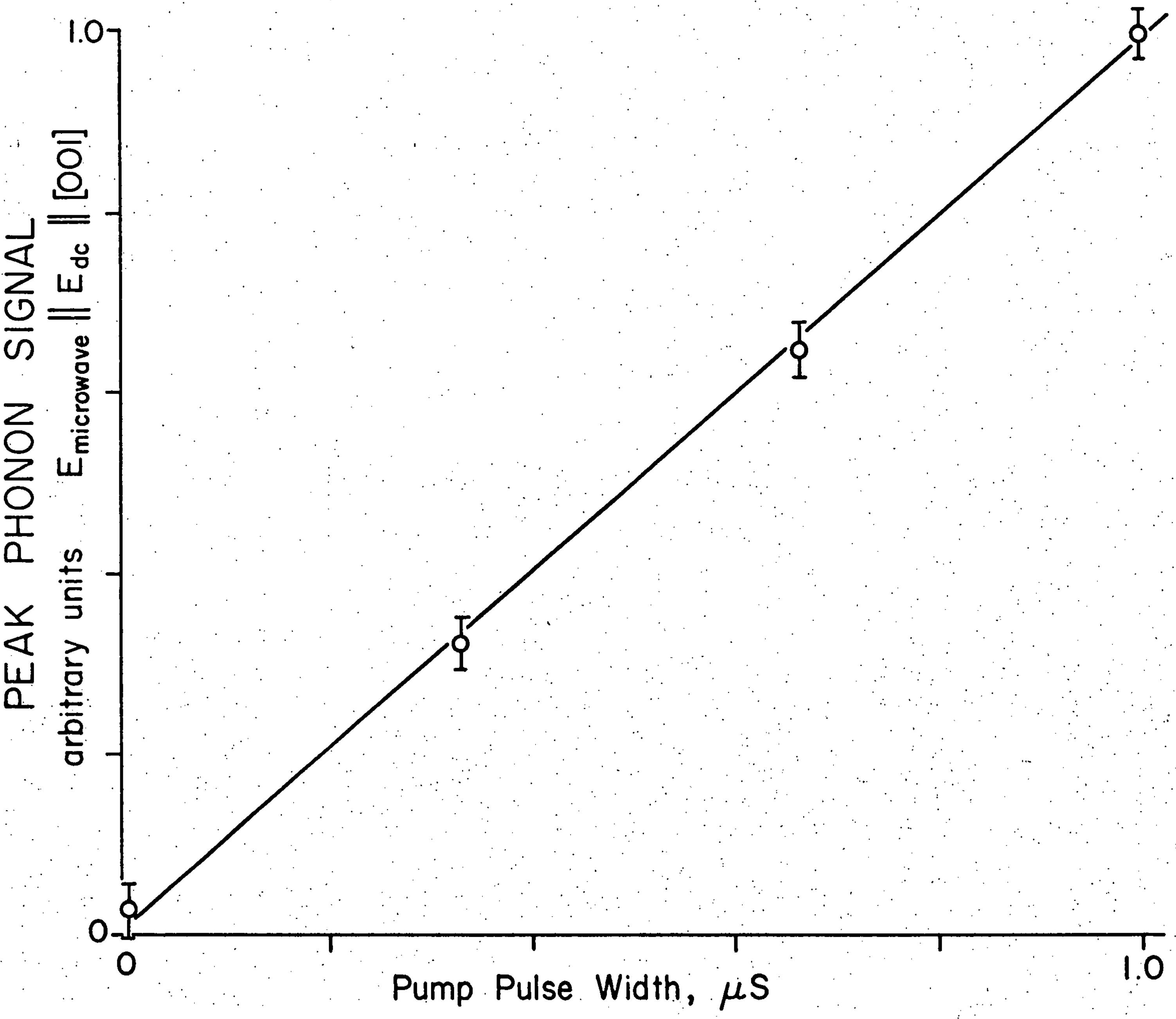
PEAK PHONON SIGNAL
arbitrary units
$E_{microwave} \parallel E_{dc} \parallel [001]$
1.0
0
0
1.0
Pump Pulse Width, μS

Figure 6.

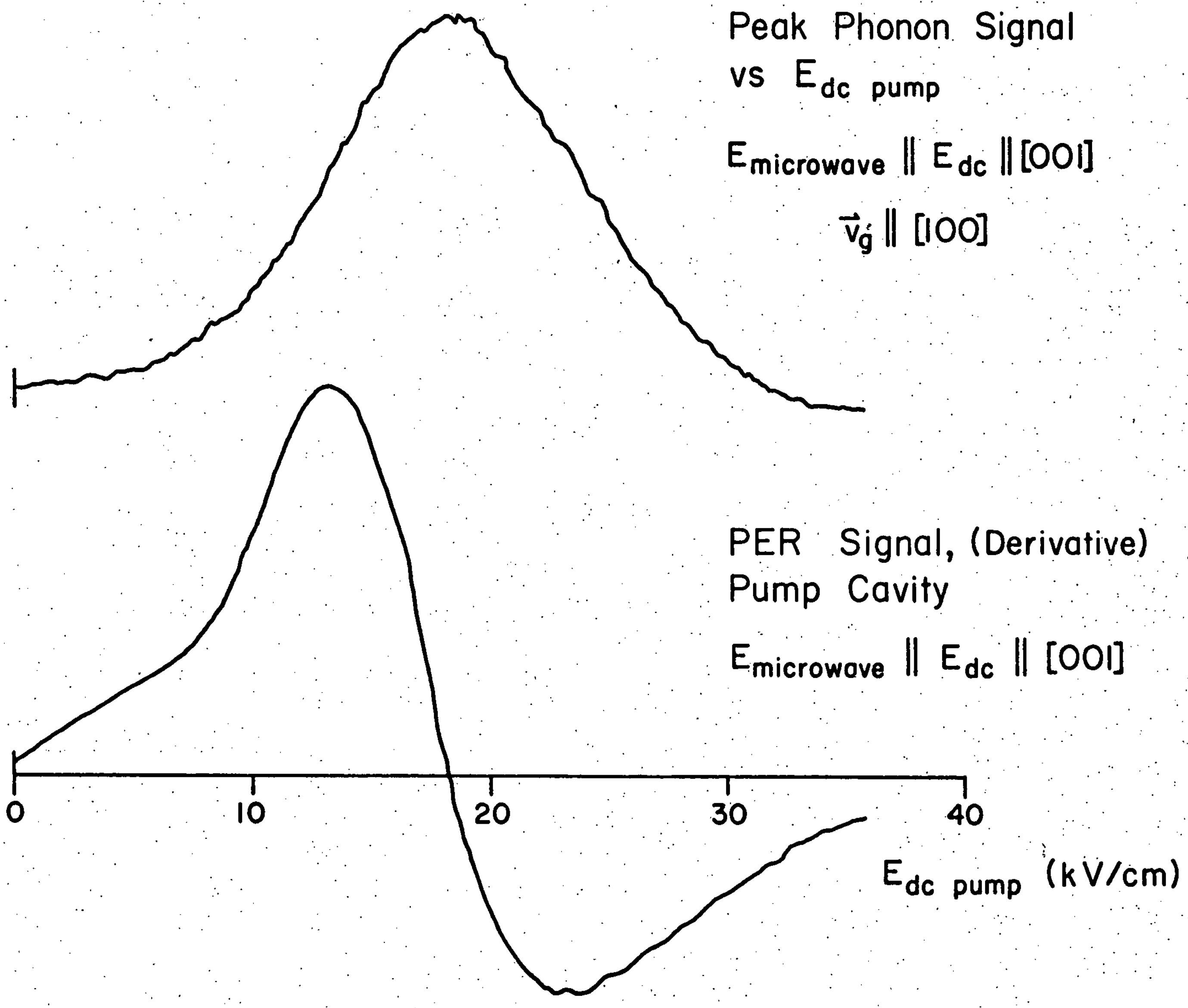
Peak Phonon Signal
vs $E_{dc\ pump}$
$E_{microwave} \parallel E_{dc} \parallel [001]$
$\vec{v}_g' \parallel [100]$
PER Signal, (Derivative)
Pump Cavity
$E_{microwave} \parallel E_{dc} \parallel [001]$
0
10
20
30
40
$E_{dc\ pump}$ (kV/cm)

Figure 7.

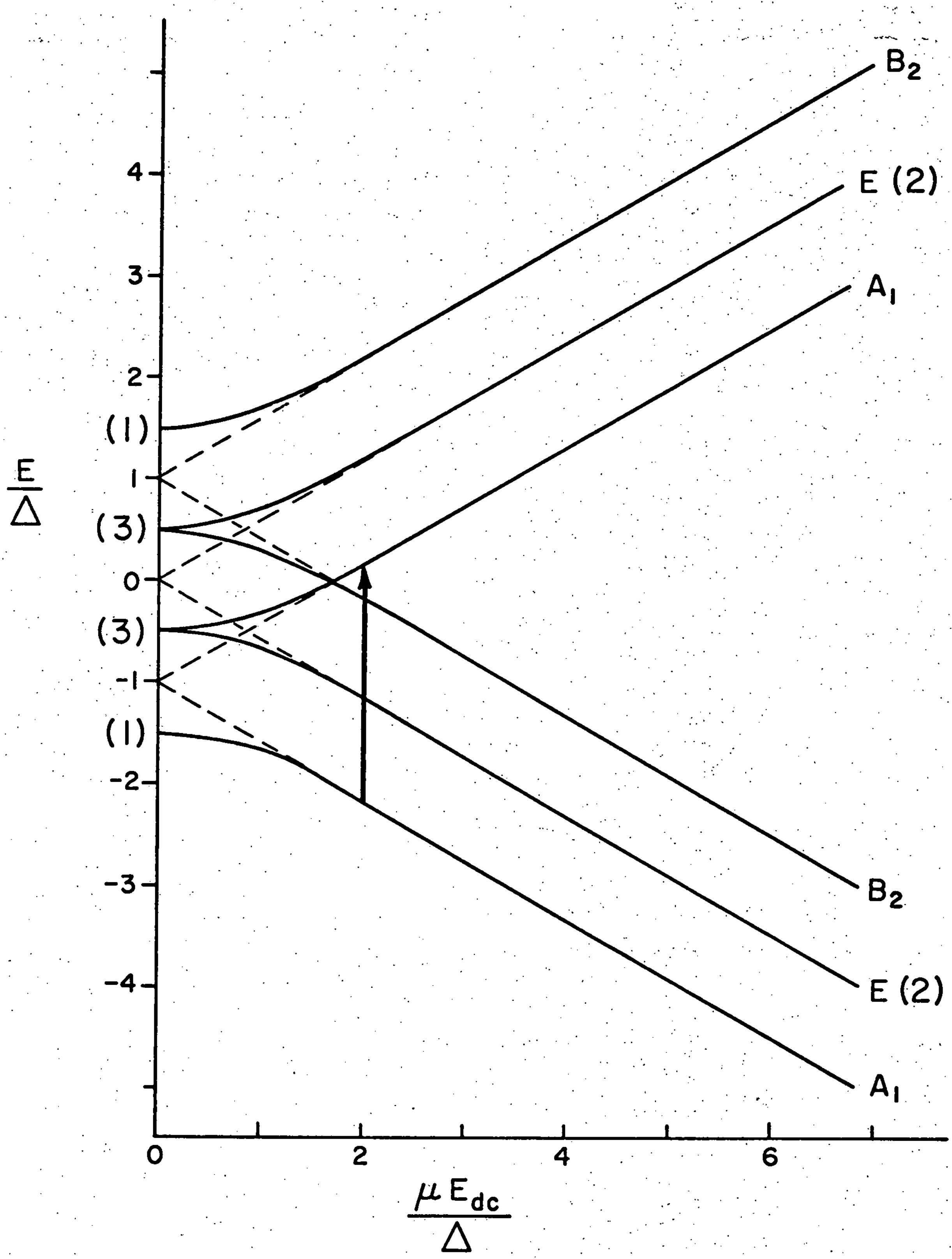

$\frac{E}{\Delta}$
4
3
2
(1)
1
(3)
0
(3)
-1
(1)
-2
-3
-4
B_2
E (2)
A_1
B_2
E (2)
A_1
0
2
4
6
$\frac{\mu E_{dc}}{\Delta}$

Figure 8a.

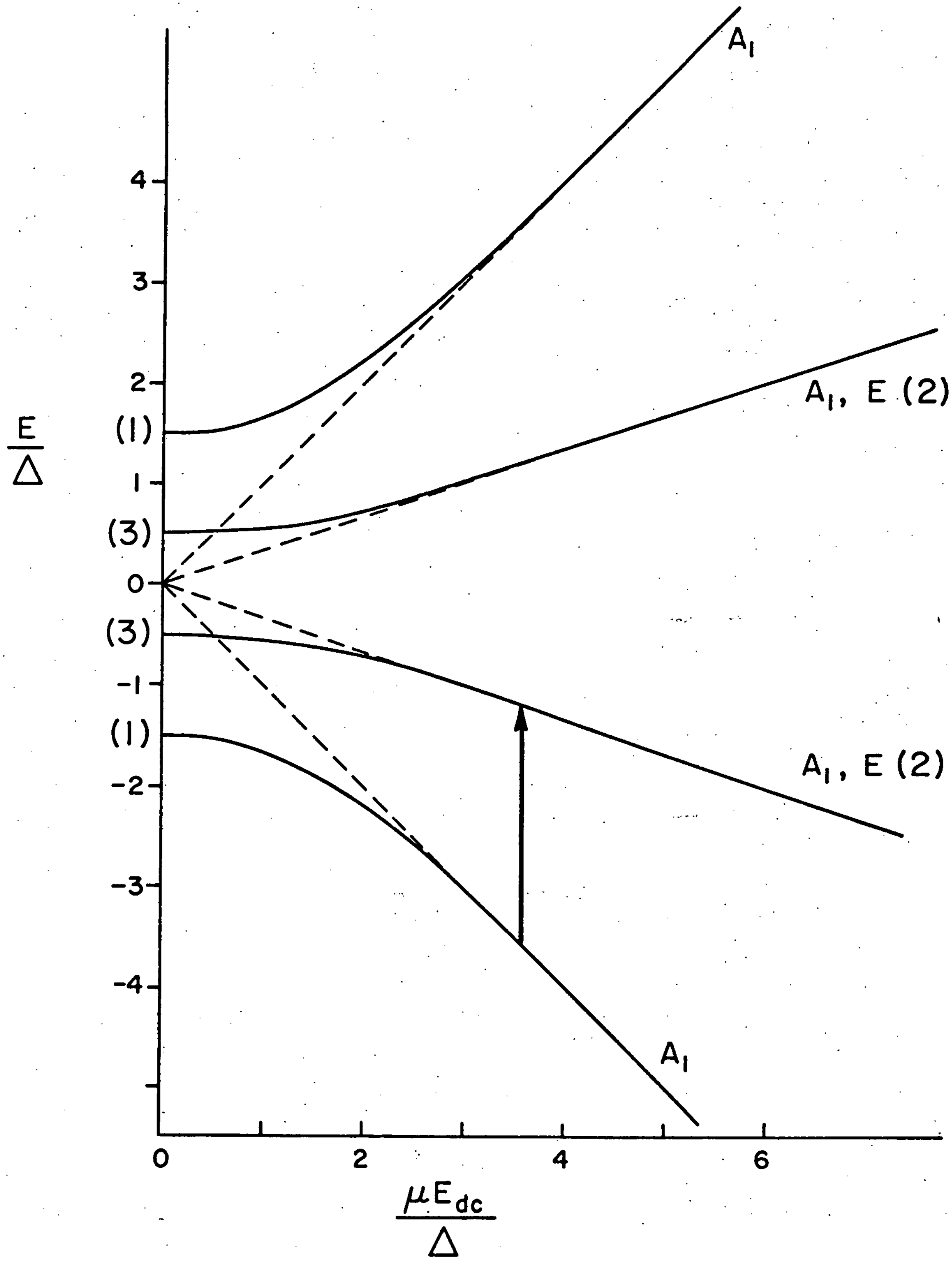

Figure 8b.